Supporting Information

Activating PtRu with Rare Earth Alloying for Efficient Electrocatalytic Methanol Oxidation Reaction

Chang Sun[a,b], Yuyan Liu[a], Zhaolei Liang[a], Qingqing Li[c*], Yaping Du[a*], Jin-Cheng Liu[a*], Yahui Cheng[b*], Feng Luo[a*]

[a]Tianjin Key Lab for Rare Earth Materials and Applications, Center for Rare Earth and Inorganic Functional Materials, School of Materials Science and Engineering, National Institute for Advanced Materials, Nankai University, Tianjin 300350, China.

[b]Department of Electronic Science and Engineering and Tianjin Key Laboratory of Process Control and Green Technology for Pharmaceutical Industry, Nankai University, Tianjin 300350, China.

[c]Hohai University, College of renewable energy, Nanjing 211100, China

Corresponding authors

Qingqing Li

Email: 1120190433@mail.nankai.edu.cn

Yaping Du

Email: ypdu@nankai.edu.cn

Jin-Cheng Liu

Email: liujincheng@nankai.edu.cn

Yahui Cheng

Email: chengyahui@nankai.edu.cn

Feng Luo

Email: feng.luo@nankai.edu.cn

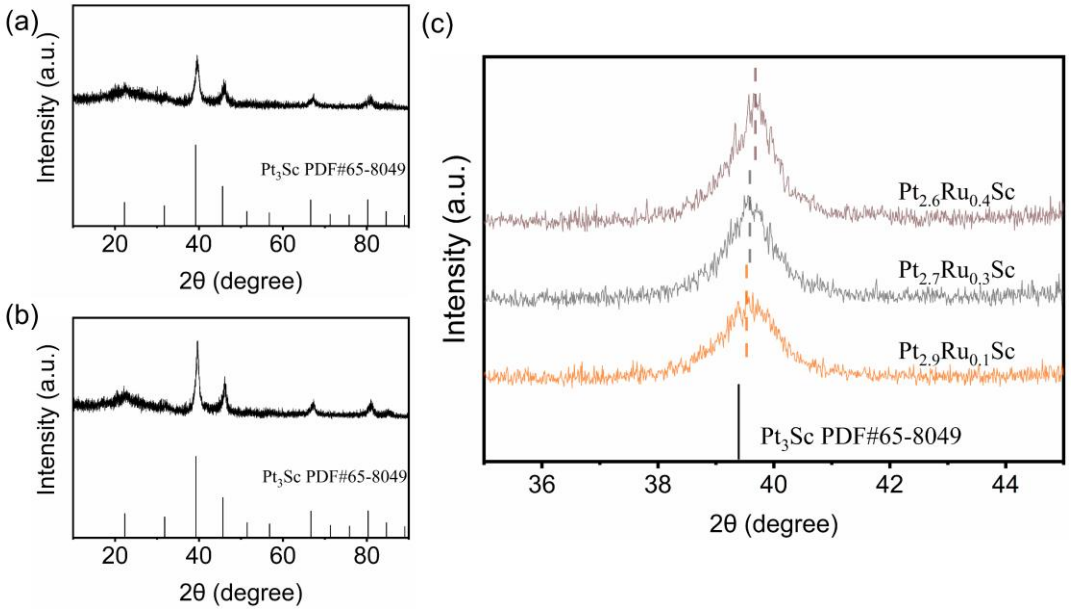

Fig. S1. XRD patterns of (a) $Pt_{2.9}Ru_{0.1}Sc$, (b) $Pt_{2.6}Ru_{0.4}Sc$, (c) enlarged 2θ range of 35−45°.

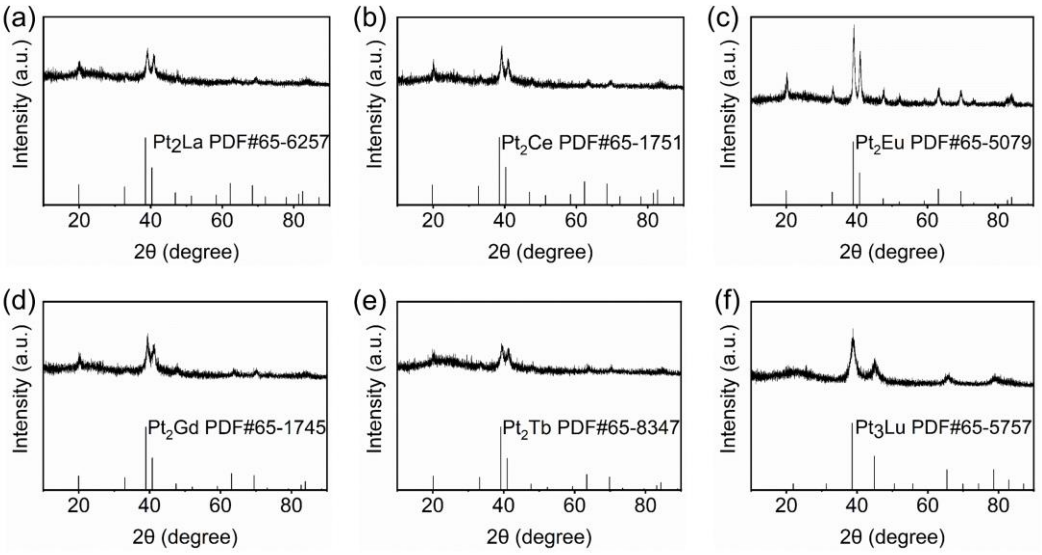

Fig. S2. XRD patterns of (a) $Pt_{1.8}Ru_{0.2}La$, (b) $Pt_{1.8}Ru_{0.2}Ce$, (c) $Pt_{1.8}Ru_{0.2}Eu$, (d) $Pt_{1.8}Ru_{0.2}Gd$, (e) $Pt_{1.8}Ru_{0.2}Tb$, (f) $Pt_{2.7}Ru_{0.3}Lu$.

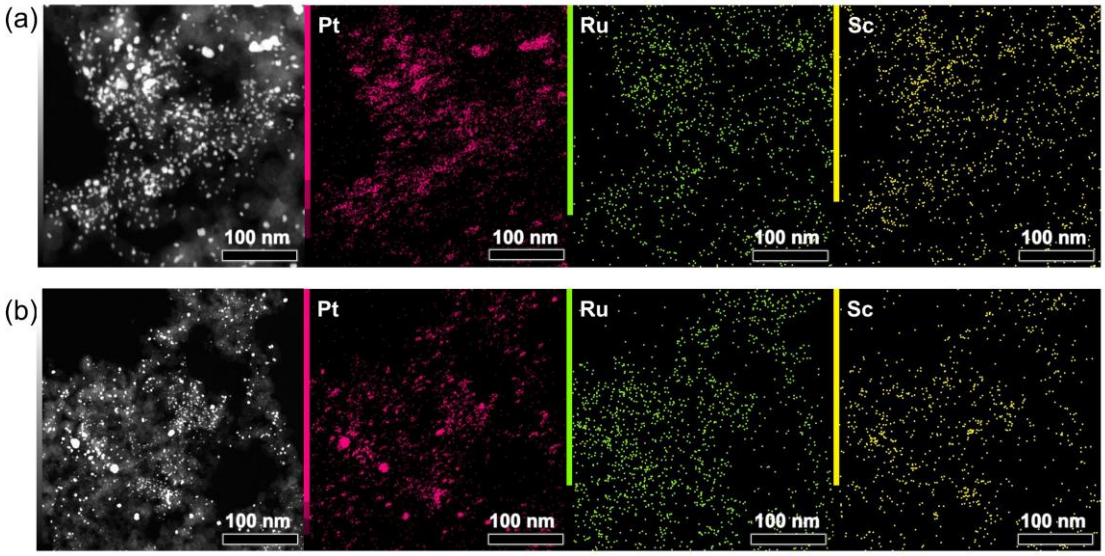

Fig. S3. EDS mappings of (a) $Pt_{2.9}Ru_{0.1}Sc$, (b) $Pt_{2.6}Ru_{0.4}Sc$.

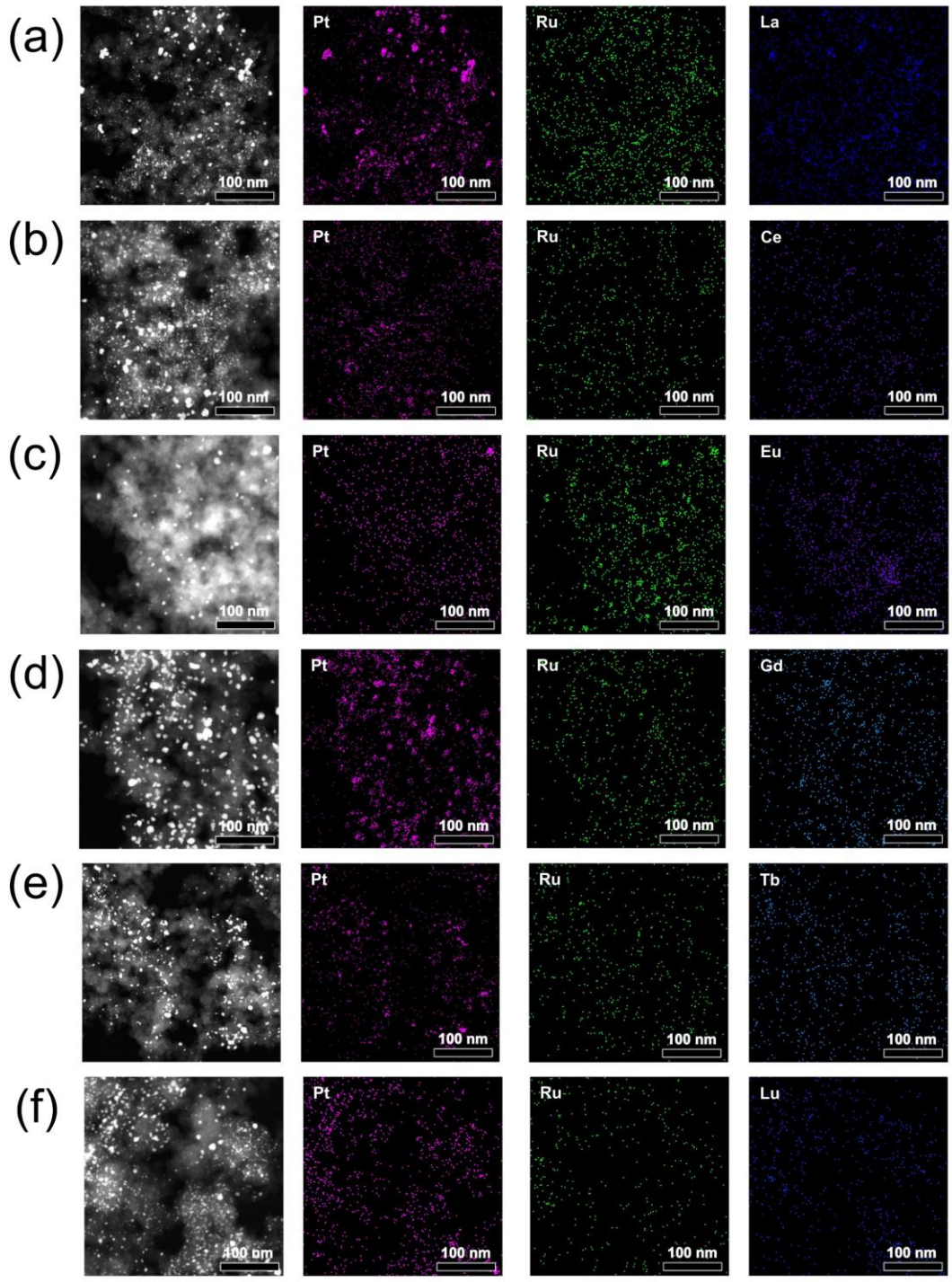

Fig. S4. EDS mappings of (a) $Pt_{1.8}Ru_{0.2}La$, (b) $Pt_{1.8}Ru_{0.2}Ce$, (c) $Pt_{1.8}Ru_{0.2}Eu$, (d) $Pt_{1.8}Ru_{0.2}Gd$, (e) $Pt_{1.8}Ru_{0.2}Tb$, (f) $Pt_{2.7}Ru_{0.3}Lu$.

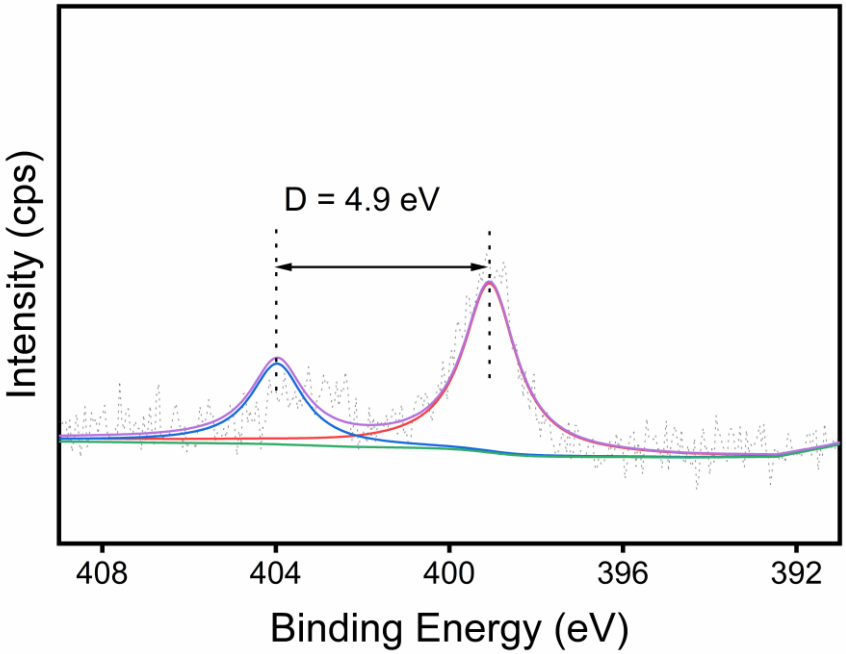

Fig. S5. Sc 2P XPS spectra of $Pt_{2.7}Ru_{0.3}Sc$

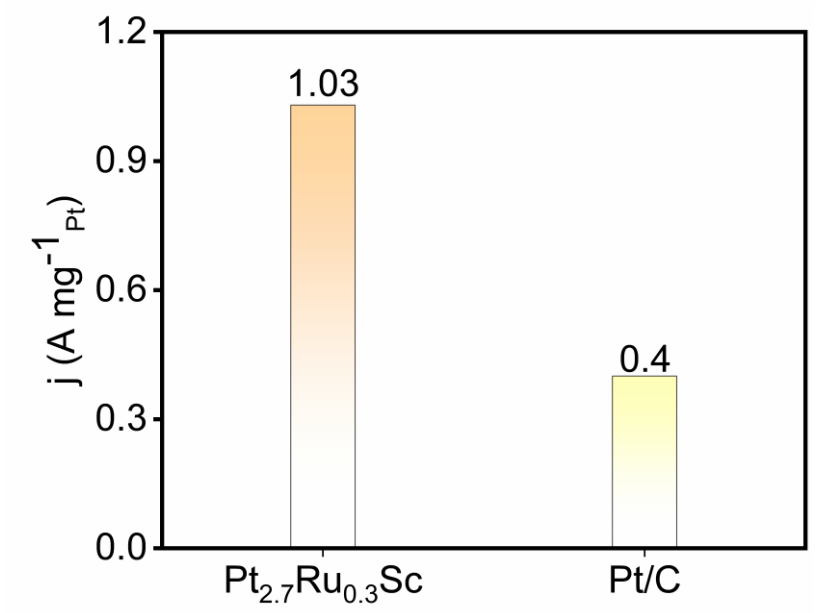

Fig. S6. Histograms of the mass activities of different catalysts.

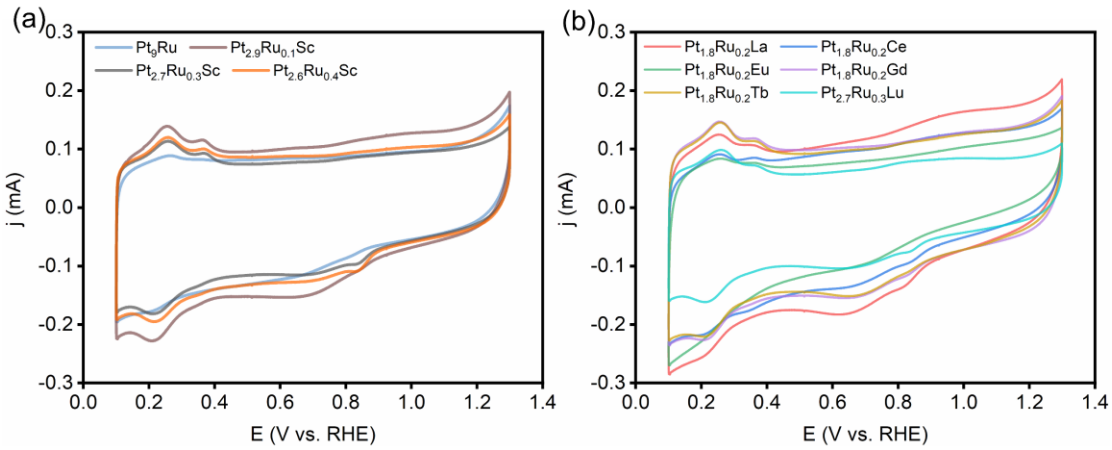

Fig. S7. (a) and (b) CVs on different catalysts at 50 mV s^{-1} in 1 M KOH solution.

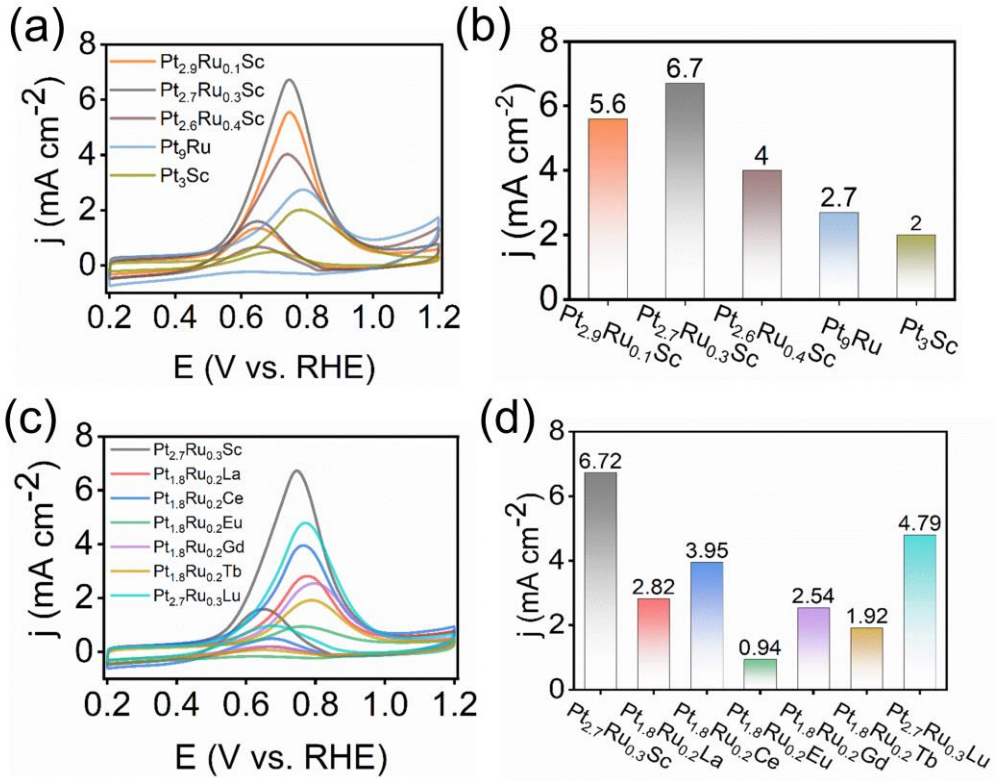

Fig. S8. (a) and (c) CVs on different catalysts at 50 mV s^{-1} for MOR in 1 M KOH + 1 M CH_3OH solution. (b) and (d) Histograms of the specific activities of different catalysts.

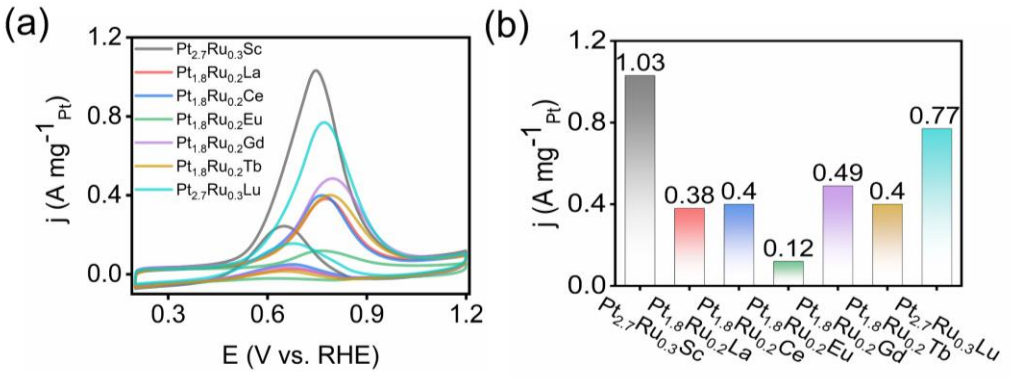

Fig. S9. (a) CVs on different catalysts at 50 mV s^{-1} for MOR in 1 M KOH + 1 M CH_3OH solution. (b) Histograms of the mass activities of different catalysts.

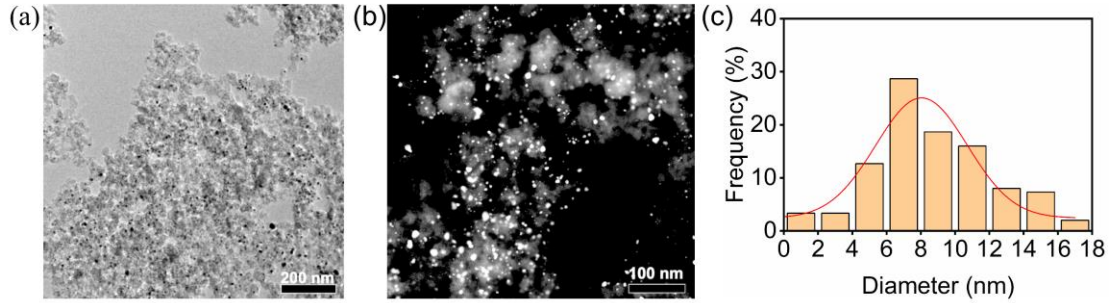

Fig. S10. (a) and (b) TEM image and (c) size distribution of $Pt_{2.7}Ru_{0.3}Sc$ after reaction.

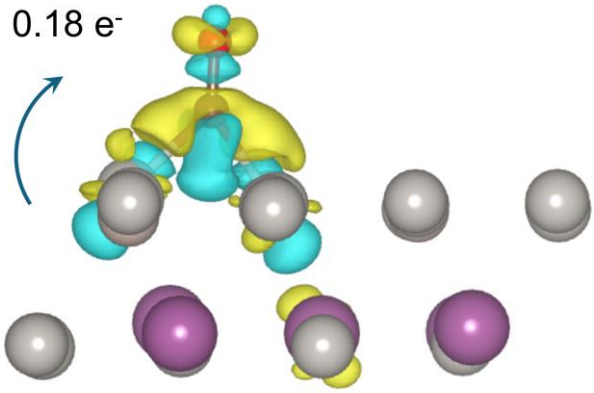

Fig. S11. Charge density difference plot of CO adsorption on PtRuSc alloy and the transferred electrons between *CO and Pt species calculated by Bader charge analysis. Yellow isosurfaces denote where electron density increases, and blue isosurfaces denote where electron density decreases.

Table S1. ICP test results for sample.

Catalysts	Pt (μg ml^{-1})	Ru (μg ml^{-1})	Sc(μg ml^{-1})
$Pt_{2.9}Ru_{0.1}Sc$	20.8	0.354	1.56
$Pt_{2.7}Ru_{0.3}Sc$	20.6	1.16	2.05
$Pt_{2.6}Ru_{0.4}Sc$	23.4	1.88	1.66
Pt_9Ru_9	21.4	1.01	-

Table S2. Comparisons of the MOR performance in previously published papers.

Catalysts	MA (A mg_{pt}^{-1})	SA (mA cm^{-2})	References
$Pt_{2.7}Ru_{0.3}Sc$	1.03	6.7	This work
$Pt_4Ru_1Cu_5$	2.07	4.1	1
PtRu NWs	0.82	1.16	2
Pt_3Co NW/C	1.95	1.55	3
PtRuLu	0.63	0.265	4
PtRuFe	1.33	1.00	5

Reference

1 H. Wang, Y. Wu, X. Luo, L. Jiao, X. Wei, W. Gu, D. Du, Y. Lin and C. Zhu, Nanoscale, 2019, 11, 10575-10580.

2 L. Huang, X. Zhang, Q. Wang, Y. Han, Y. Fang and S. Dong, Journal of the American Chemical Society, 2018, 140, 1142-1147.

3 L. Bu,S. Guo,X. Zhang,X. Shen,D. Su,G. Lu,X. Zhu,J. Yao,J. Guo,X. Huang, *Nature Communications* **2016,** *7*.

4 Y. Cheng,H. Wang,T.-W. Jiang,X. Guo,F. Kwofie,H. Su,L. Khotseng,W. Zeng,Y. Zhang,Y. Liu,W.-B. Cai,S. Wang, Acs Applied Materials & Interfaces 2024, 16, 20352-20359

5 Y. Ren, S. Askarov, Y. Zhang, D. Shi, Q. Wu, K. Chen and H. Li, Journal of Alloys and Compounds, 2024, 978, 173442.